ISSN(Online): 2320-9801
ISSN (Print) : 2320-9798

International Journal of Innovative Research in Computer and Communication Engineering

(An ISO 3297: 2007 Certified Organization)

Vol. 4, Issue 6, June 2016

ANN Based DC-DC Converter for Renewable Energy Based Servo Drives

Ramakrishnaprabu.G [1], Ramesh.T[2]

Associate Professor, Dept. of. EEE, VMKV Engineering College, Salem, Tamilnadu, India[1]

PG Student [PSE], Dept. of EEE, VMKV Engineering College, Salem, Tamilnadu, India[2]

ABSTRACT: Now days the electric power utility is raised due to the presence of more no of peoples, if it is continued one day the power demand may increase, hence the new kind of source investigation is essential to build our live style effectively. Recently the Renewable energy source is identified as a alternative for conventional electric source. The renewable energy such as Wind and Photo-Voltaic (PV) arrays are widely using in automobiles, industries, residential and commercial buildings, all the systems energy storage devices are required for backup the power. Hence I would like to propose the renewable energy based servo drives.In the Proposed system the Full bridge with three port converters based systematic method is developed. The MOSFET hex bridge consists of two bidirectional ports and an isolated output port. The primary circuit of the converter functions as a boost converter and provides a power flow path between the ports on the primary side. The three port converter features single stage conversion between any two of the three ports and closed loop with feedback circuit. Its result is higher system efficiency, fewer components, faster response and compact packaging. The Boost converter can adapt to a wide source voltage range and servo drive runs at constant speed for various load conditions by using the ANN controller.

KEYWORDS: Photovoltaic, Full Bridge with three port network, Servo Drive, Artifical Neural Network (ANN)

I. INTRODUCTION

Fully isolated MPCs are typically derived by combining full-bridge, half-bridge, or series-resonant topologies via magnetic coupling, e.g., utilizing multi winding transformers. Isolation and bidirectional capabilities of all the ports and ZVS can be achieved in these topologies. These MPCs are good candidates for the applications where isolation and bidirectional conversion are required. However, the major problem is that too many active switches are used. This results in complicated driving and control circuitry, which may degrade the reliability and performance of the integrated converters. Non isolated MPCs can either be derived by using dc-link or integration method. These MPCs feature compact design and high power density. However, voltage levels of all ports are not flexible, and ZVS cannot be achieved easily. Partly isolated MPCs are based on hybrid topologies of isolated circuits and non-isolated circuits, which can provide the necessary isolation for the load with flexible voltage levels and maintain advantages of compact design and high power density. A boost-integrated MPC has been presented by combining a PS-FBC and a boost converter. The power flow control has been realized by using PWM plus phase-angle-shift control scheme. This principle is further applied to the three-phase FBC. These MPCs have some common features, i.e., the structures of the primary side circuit are similar. However, they have only rarely been examined and investigated in terms of their relationships, topological characteristics, or how to derive these topologies.

The main focus of this paper is to propose a systematic method for the derivation of MPC topologies from FBC and non-isolated BDCs. The derived MPCs, provide good candidates for the applications of renewable power system, such as PV-supplied aerospace power systems, hybrid energy storage systems, fuel cell and battery systems, and thermoelectric generation systems with battery backup.

ISSN(Online): 2320-9801
ISSN (Print) : 2320-9798

International Journal of Innovative Research in Computer and Communication Engineering

(An ISO 3297: 2007 Certified Organization)

Vol. 4, Issue 6, June 2016

II. BLOCK DIAGRAM

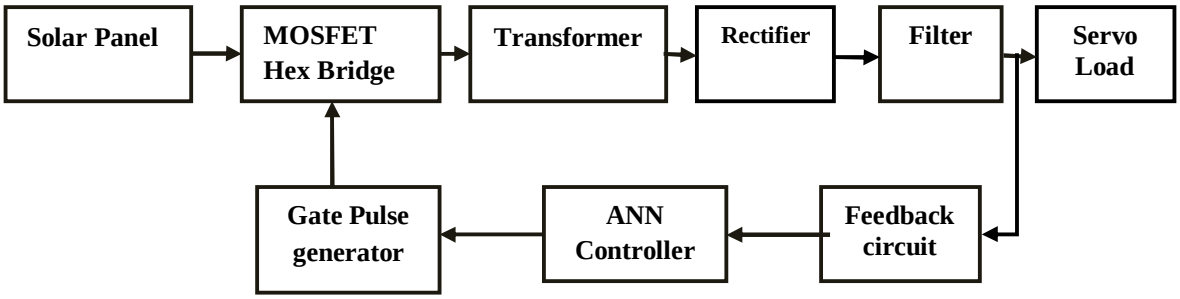

Fig 1 Block Diagram

Explanation

The fig 1 shows the block diagram of the proposed method. By using the method the servo load runs with the constant input.The solar output is taken to the feedback circuit and to the ANN.The ANN compares the instantaneous value of the panal with the reference value.If the Error is zero the output of the panel is taken to the servo load otherwise the gate pulse is adjusted to drive the MOSFET bridge to made the instant value make it comfort to the load.

III. DERIVATION OF THE FB-BDC-MPC TOPOLOGIES

Topologies of the FB-BDC-MPCs

1) Three-Port Converter Family:

By combining the two BDCs in parallel, the derived FB-BDC-MPC topologies have three ports totally, and a family of three-port converters can be harvested. In each of the resulted topologies, both the two sources, $U1$ and $U2$, can supply power to the load, Uo, and the power can also be exchanged simultaneously between $U1$ and $U2$ under control because the primary side of the converter features a BDC.

2) Four-Port Converter Family:

By combining the twoBDCs with a port shared, the derived FB-BDC-MPC topologies have four ports totally, and a family of four-port converter scan be harvested. In each of the resulted topologies, all the three sources, $U1$, $U2$, and $U3$, can supply power to the load, Uo, and the power can also be exchanged simultaneously between $U1$ and $U2/U3$ because the two BDCson the primary side of the converter build a bidirectional three port converter. Single-stage conversion between $U1$ and $U2$ and$U1$ and $U3$ can be achieved with the bidirectional three-portconverter on the primary side. However, the conversion between$U2$ and $U3$ is a two-stage one.

3) **Five-Port Converter Family:**

By combining the twoBDCs with only a terminal shared, the derived FB-BDC-MPCtopologies have five ports totally, and a family of five-port converters can be harvested. In each of the resulted topologies, all the four sources, $U1$, $U2$, $U3$, and $U4$,can supply power to the load, Uo, and the power can also be exchanged simultaneously between $U1$ and $U2$ and $U3$ and $U4$under control because the primary side of the converter features two BDCs. However, $U1$ and $U2$ cannot directly exchange power with $U3$ and $U4$ because the two BDCs on the primary sides are independent of each other.

ISSN(Online): 2320-9801
ISSN (Print) : 2320-9798

International Journal of Innovative Research in Computer and Communication Engineering

(An ISO 3297: 2007 Certified Organization)

Vol. 4, Issue 6, June 2016

ANALYSIS ON THE BB-FPC

The switches $S1$ and $S2$ and the inductor $L1$form a boost converter to interface the PV panel PV1 with the battery. The switches $S3$ and $S4$ and the inductor $L2$ form another boost converter to interface the PV panel PV2 with the battery. Since the equivalent circuit from PV to the battery is a boost converter, the PV voltage must be lower than the battery voltage. In addition, the switches $S1$ –$S4$, the transformer T, the output diodes $Do1$ –$Do4$, the output filter inductor Lo, and the output capacitor Co compose a PS-FBC, which can supply power to the isolated load uo.

SWITCHING STATE

The two switches of each leg are operated in complementary to generate a rectangular voltage from the midpoint of the leg. Duty cycles of S2(S1) and S4(S3) are adopted as two control variables to control the power exchanging between the PV1 and the battery and the PV2 and the battery, respectively. Furthermore, the two rectangular-wave voltages, uaand ub, the outputs from the midpoints of the two legs, are in phase shift with an angle ϕto control and regulate the output voltage Uo. Define the turn's ratio of the transformer as NP: NS = 1: n and the voltage on the block capacitor Cbas UCb. There are six switching states in one switching cycle.

Mode I [t0 –t1]:

At t0, S1 is turned off, S2 is turned on, and S3 remains on. L1 begins to be charged, and L2 is still discharged linearly. The filter inductor current, iLo, freewheels through the rectifier diodes,Do1–Do4, and the secondary windings of the transformer is shorted by the rectifier diodes

diP / dt= −(Ub+ UCb) / Lk

Mode II [*t*1 − *t*2]:

At *t*2, *ip*= −*ni*Lo, and *Do*1 and *Do*4 bear reverse bias. The primary sources supply power to the load through the transformer. The important equations of this state are as follows:

$Di_{L1}/dt= U_{PV1}/L1$

$di_{L2}/dt= (U_{PV2}-U_b)/L_2$

$di_{Lo}/dt= (n[Ub+UCb]-Uo)/Lo$

The drain-to-source currents through *S*2 and *S*3 are

iS2(t) = iL1(t) + niLo(t)

iS3(t) = −iL2(t) + niLo(t).

Mode III [*t*2 − *t*3]:

At *t*2, *S*3 is turned off, *S*4 is turned on, and *S*2 remains on. *iL*2 starts to increase, and the voltage of the block capacitor *Cb*, *U*Cb, applies on the transformer primary windings

$di_{L1}/dt= U_{PV1}/L1$

$di_{L2}/dt=$ UPV2/L2

diLo/dt= (nUCb−Uo)/Lo

The drain-to-source current through *S*4 is

*iS*4(*t*) = *iL*2(*t*) − *ni*Lo(*t*).

Mode IV [*t*3 − *t*4]:

At *t*3, *S*2 is turned off,*S*1 is turned on, and *S*4 remains on. *L*1 begins to be discharged, and*L*2 is still charged linearly. *i*Lo begins to freewheel throughthe rectifier diodes, *Do*1 − *Do*4, and the voltage applied on theleakage inductance *Lk*is (*Ub*− *U*Cb)

diP /dt= (Ub– Ucb)/ Lk

Mode V [*t*4 − *t*5]:

In this state, *Do*2 and*Do*3 bear reverse bias. The filter inductor current *i*Lo fully flowsthrough *Do*1 and *Do*4

diL1/dt= (UPV1−Ub) /L1

ISSN(Online): 2320-9801
ISSN (Print) : 2320-9798

International Journal of Innovative Research in Computer and Communication Engineering

(An ISO 3297: 2007 Certified Organization)

Vol. 4, Issue 6, June 2016

diL2/dt= UPV2/L2
diLo/dt= (n[Ub−UCb]−Uo)/Lo
The drain-to-source currents through *S*1 and *S*4 are

$iS2(t) = -iL1(t) + niLo(t)$
$iS4(t) = iL2(t) + niLo(t)$

Mode VI [t5 − t6]:

At t5, S4 is turnedoff, S3 is turned on, and S1 remains on. UCb applies on thetransformer primary windings, iL2 begins to decrease, and iLoflows through Do1 and Do4
diP/dt= −UCb/Lk
diL1/dt= (UPV1−Ub)/L1
diL2/dt= (UPV2−Ub)/L2
diLo/dt= −Uo/Lo
The drain-to-source current through S3 is
iS4(t) = −iL2(t) − niLo(t)
This state ends until *S*1 is turned off and *S*2 is turned on. Then,a new switching period begins.

III CIRCUIT DIAGRAM

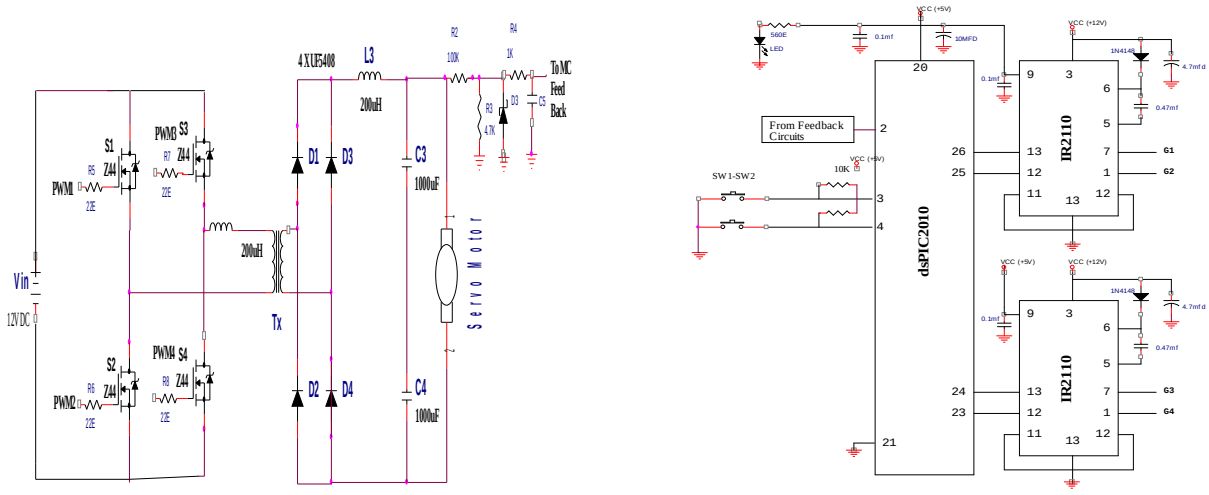

Fig 2 Circuit Diagram

Digital signal controller used to create PWM pulse and it also controls closed loop algorithm using ANN.DSC operating voltage is 5 Volt. So it will be operate at 5V logic. But MOSFET operates at 12V Logic Level. So we want 5V logic Level to 12V Logic Level. For this purpose we use IR2110.A digital signal controller (DSC) can be thought of as a hybrid of microcontrollers and digital signal processors (DSPs).The 30 MIPS dsPIC30F family is developed for applications that benefit from a wide operating voltage (2.5 to 5.5V), extremely low standby current, integrated EEPROM, and for those that prefer 5V operation due to system considerations.

ISSN(Online): 2320-9801
ISSN (Print) : 2320-9798

International Journal of Innovative Research in Computer and Communication Engineering

(An ISO 3297: 2007 Certified Organization)

Vol. 4, Issue 6, June 2016

IV RESULTS AND DISCUSSIONS

Experimental results will give 100-W prototype of BB-FPC with good steady-state and dynamic performances demonstrate the feasibility and effectiveness of the proposed method with help of ANN controller.

S.no	Input Voltage in Volts	Load Current In amps	Output Voltage in Volts		% of Efficiency(avg)	
			Open Loop	Closed Loop	Open loop	Closed Loop
1	15.4	0.2	22.0	25.6	60	96
2	15.6	0.3	21.5	25.3	60	96
3	15.3	0.5	20.0	25.2	60	96
4	15.5	0.8	18.3	25.2	60	96
5	16.0	1.0	17.6	25.0	60	96

Table 1 Result

INPUT VOLTAGE **OUTPUT VOLTAGE**

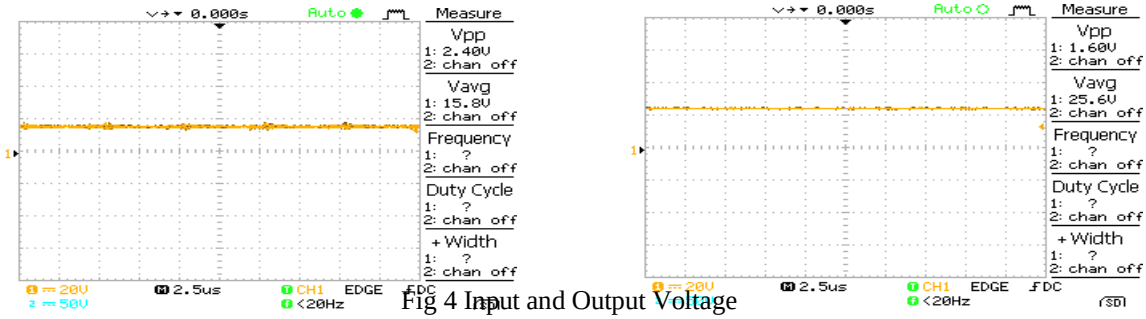

Fig 4 Input and Output Voltage

In the above fig the input and output voltages are shown

GATE PULSE AT OPEN LOOP **OUTPUT VOLTAGE AT OPEN LOOP**

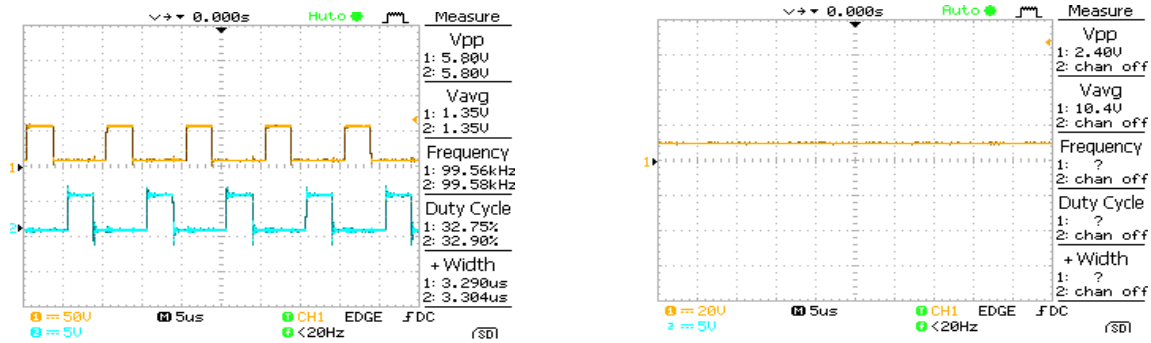

Fig 5 Gate Pulse and Output Voltage at Open Loop

The fig 5 shows the gale and output voltage for the open loop system.

ISSN(Online): 2320-9801
ISSN (Print) : 2320-9798

International Journal of Innovative Research in Computer and Communication Engineering

(An ISO 3297: 2007 Certified Organization)

Vol. 4, Issue 6, June 2016

GATE PULSE AT CLOSED LOOP **OUTPUT VOLTAGE AT CLOSED LOOP**

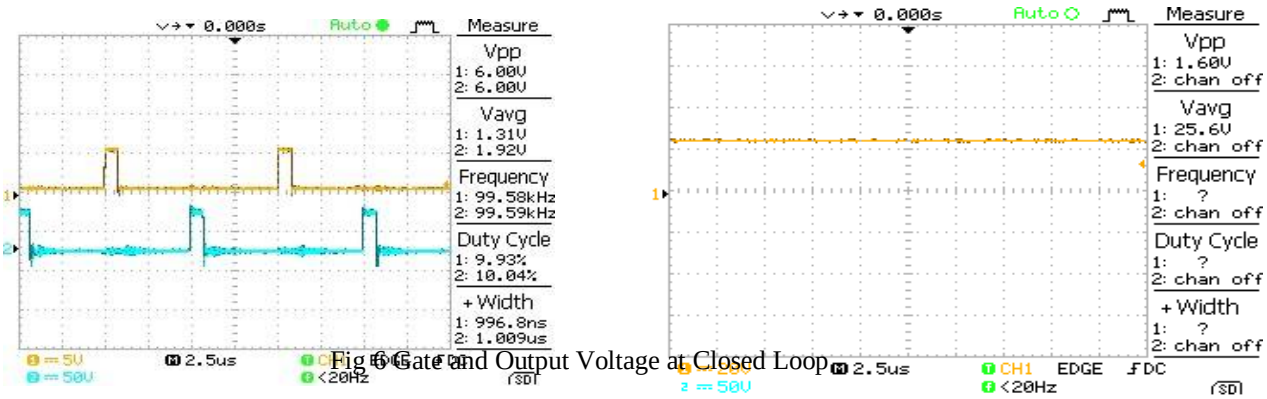

Fig 6 Gate and Output Voltage at Closed Loop

The above results give better result in closed loop compare than open loop. Here we give prototype model for 12V to 24V boost converter.

V. CONCLUSION

A systematic method for synthesizing MPCs from FBC and BDCs has been proposed. The switching legs parasitized in the BDCs have been found and shared with theFBC to derive families of FB-BDC-MPCs. The proposed FBBDC-MPCs are capable of interfacing multiple bidirectional sources and isolated output load simultaneously. Single-stage power conversion between any two ports and ZVS of all the active switches have been achieved in the proposed MPCs.These result in high conversion efficiency. All the port voltages are controlled simultaneously by employing PWM and phase angle-shift control scheme. These topologies are good candidates for renewable power systems as interface converters due to their advantages of simple configuration, reduced devices, and easy control.A typical four-port converter developed by the proposed method, named as BB-FPC, is analyzed and implemented as an example, with detailed operation principles, design considerations, modulation, and power management strategies presented. Experimental results on a 100-W prototype of BB-FPC with good steady-state and dynamic performances demonstrate the feasibility and effectiveness and runs the servo drives runs at a constant speed of the proposed method.

REFERENCES

[1] H. Fakham, D. Lu, and B. Francois, "Power control design of a battery charger in a hybrid active PV generator for load-following applications," *IEEE Trans. Ind. Electron.*, vol. 58, no. 1, pp. 85–94, Jan. 2011.
[2] T. Hirose and H. Matsuo, "Standalone hybrid wind-solar power generation system applying dump power control without dump load," *IEEE Trans. Ind. Electron.*, vol. 59, no. 2, pp. 988–997, Feb. 2012.
[3] W. Jiang and B. Fahimi, "Multiport power electronic interface—Concept, modeling and design," *IEEE Trans. Power Electron.*, vol. 26, no. 7, pp. 1890–1900, Jul. 2011.
[4] H. Tao, J. L. Duarte, and M. A. M. Hendrix, "Multiport converters for hybrid power sources," in *Proc. IEEE PESC*, 2008, pp. 3412–3418.
[5] H. Tao, J. L. Duarte, andM. A.M. Hendrix, "Three-port triple-half-bridge bidirectional converter with zero-voltage switching," *IEEE Trans. Power Electron.*, vol. 23, no. 2, pp. 782–792, Mar. 2008.
[6] H. Tao, A. Kotsopoulos, J. Duarte, andM. Hendrix, "Transformer coupled multiport ZVS bidirectional dc-dc converter with wide input range," *IEEE Trans. Power Electron.*, vol. 23, no. 2, pp. 771–781, Mar. 2008.
[7] K. Haribaran and N. Mohan, "Three-port series-resonant dc-dc converter to interface renewable energy sources with bidirectional load and energy storage ports," *IEEE Trans. Power Electron.*, vol. 24, no. 10, pp. 2289– 2297, Oct. 2009.
[8] T. Zhou and B. Francois, "Energy management and power control of a hybrid active wind generator for distributed power generation and grid integration," *IEEE Trans. Ind. Electron.*, vol. 58, no. 1, pp. 95–104, Jan. 2011.
[9] T. Bhattacharya, V. S. Giri, K. Mathew, and L. Umanand, "Multiphase bidirectional flyback converter topology for hybrid electric vehicles," *IEEE Trans. Ind. Electron.*, vol. 56, no. 1, pp. 78–84, Jan. 2009.
[10] X. Liu, P. Wang, P. C. Loh, and F. Blaabjerg, "A compact three-phase single-input/dual-output matrix converter," *IEEE Trans. Ind. Electron.*, vol. 59, no. 1, pp. 6–16, Jan. 2012.
[11] R.-J. Wai, C.-Y. Lin, J.-J. Liaw, and Y.-R. Chang, "Newly designed ZVS multi-input converter," *IEEE Trans. Ind. Electron.*, vol. 58, no. 2, pp. 555–566, Feb. 2011.
[12] L. D. Salazar and J. R. Urra, "A novel three ports power conditioner for renewable electricity generators," in *Proc. IEEE IECON*, 2011, pp. 1131–1136.

ISSN(Online): 2320-9801
ISSN (Print) : 2320-9798

International Journal of Innovative Research in Computer and Communication Engineering

(An ISO 3297: 2007 Certified Organization)

Vol. 4, Issue 6, June 2016

[13] H. Matsuo, W. Lin, F. Kurokawa, T. Shigemizu, and N. Watanabe, "Characteristics of the multiple-input dc-dc converter," *IEEE Trans. Ind. Electron.*, vol. 51, no. 3, pp. 625–631, Jun. 2004.
[14] P. Gules, J. De Pellegrin Pacheco, H. L. Hey, and J. Imhoff, "A maximum power point tracking system with parallel connection for PV stand-alone applications," *IEEE Trans. Ind. Electron.*, vol. 55, no. 7, pp. 2674–2683, Jul. 2008.